Journal of Inflammation Research

Dovepress
open access to scientific and medical research

Open Access Full Text Article

ORIGINAL RESEARCH

Identification of Diagnostic Genes of Aortic Stenosis That Progresses from Aortic Valve Sclerosis

Chenxi Yu[1,*], Yifeng Zhang[1,*], Hui Chen[2,*], Zhongli Chen[3], Ke Yang[1]

[1]Department of Cardiovascular Medicine, Ruijin Hospital, Shanghai Jiao Tong University School of Medicine, Shanghai, 200025, People's Republic of China; [2]Department of Cardiology, Shanghai Ninth People's Hospital, Shanghai Jiaotong University School of Medicine, Shanghai, 200011, People's Republic of China; [3]State Key Laboratory of Cardiovascular Disease, Cardiac Arrhythmia Center, Fuwai Hospital, National Center for Cardiovascular Disease, Chinese Academy of Medical Sciences and Peking Union Medical College, Beijing, 100037, People's Republic of China

*These authors contributed equally to this work

Correspondence: Ke Yang, Department of cardiovascular medicine, Ruijin Hospital, Shanghai Jiaotong University School of Medicine, 197 Rui Jin Road II, Shanghai, 200025, People's Republic of China, Tel/Fax +86 21 64370045, Email ykk_ykkk@126.com; Zhongli Chen, State Key Laboratory of Cardiovascular Disease, Cardiac Arrhythmia Center, Fuwai Hospital, National Center for Cardiovascular Disease, Chinese Academy of Medical Sciences and Peking Union Medical College, Beijing, 100037, People's Republic of China, Tel/Fax +861088392295, Email zhonglichen555@126.com

Background: Aortic valve sclerosis (AVS) is a pathological state that can progress to aortic stenosis (AS), which is a high-mortality valvular disease. However, effective medical therapies are not available to prevent this progression. This study aimed to explore potential biomarkers of AVS-AS advancement.

Methods: A microarray dataset and an RNA-sequencing dataset were obtained from the Gene Expression Omnibus (GEO) database. Differentially expressed genes (DEGs) were screened from AS and AVS samples. Functional enrichment analysis, protein–protein interaction (PPI) network construction, and machine learning model construction were conducted to identify diagnostic genes. A receiver operating characteristic (ROC) curve was generated to evaluate diagnostic value. Immune cell infiltration was then used to analyze differences in immune cell proportion between tissues. Finally, immunohistochemistry was applied to further verify protein concentration of diagnostic factors.

Results: A total of 330 DEGs were identified, including 92 downregulated and 238 upregulated genes. The top 5% of DEGs (n = 17) were screened following construction of a PPI network. IL-7 and VCAM-1 were identified as the most significant candidate genes via least absolute shrinkage and selection operator (LASSO) regression. The diagnostic value of the model and each gene were above 0.75. Proportion of anti-inflammatory M2 macrophages was lower, but the fraction of pro-inflammatory gamma-delta T cells was elevated in AS samples. Finally, levels of IL-7 and VCAM-1 were validated to be higher in AS tissue than in AVS tissue using immunohistochemistry.

Conclusion: IL-7 and VCAM-1 were identified as biomarkers during the disease progression. This is the first study to analyze gene expression differences between AVS and AS and could open novel sights for future studies on alleviating or preventing the disease progression.

Keywords: aortic stenosis, aortic valve sclerosis, diagnostic genes, machine learning, immune infiltration, immunohistochemistry

Introduction

According to 2020 American College of Cardiology/American Heart Association guidelines, aortic valve sclerosis (AVS) is defined as aortic valve thickening without flow limitation and with maximum aortic velocity <2 m/s.[1] The prevalence of AVS is 25% to 30% among individuals over 65 years of age.[2] Additionally, one-third of AVS will progress to a certain degree of aortic stenosis (AS) during an average follow-up period of 4 years.[3] AS is defined as aortic valve calcification or fibrosis with a maximum aortic velocity >2 m/s.[1] AS is one of the most prevalent high-mortality valvular diseases, with a 4-year event-free survival rate of only 16%, even in asymptomatic severe AS cases.[4,5] Surgical aortic valve replacement (SAVR) and transcatheter aortic valve implantation (TAVI) can significantly decrease AS mortality.[6,7] However, surgical operations come with risks, such as infections and arrhythmias.[8,9] Unfortunately, effective medical therapies are not available to prevent

Received: 4 December 2023
Accepted: 14 May 2024
Published: 28 May 2024

the progression from AVS to AS.[10,11] Therefore, it is vital to study gene expression differences in AVS and AS and research the role of potential genes to better understand the underlying disease progression mechanism.

Previous studies have reported that inflammation contributes to the occurrence of AS and based on the development of microarray and transcriptome sequencing technology, some immune-related biomarkers distinguishing patients with AS from healthy controls have been identified.[12,13] By analyzing gene expression differences between stenosis and normal valves, Wang et al reported that chemokines, such as CXCL13, CXCL8 and CXCL16, could serve as vital markers.[14] Further, Liu et al found that MMP9, a mitochondria-related gene, was a novel biomarker and potential therapeutic target for AS.[15] Wu et al also discovered five immune-related diagnostic hub genes for AS patients with metabolic syndrome.[16] All of these studies aimed to compare stenosis and normal valves. However, limited research has been conducted to identify biomarkers during the progression from AVS to AS and to analyze changes in immune microenvironments between sclerotic and stenotic valves.

To the best of our knowledge, this is the first study to distinguish diagnostic biomarkers for the progression from AVS to AS. First, we obtained a microarray dataset and an RNA-sequencing dataset from the Gene Expression Omnibus (GEO) database, both of which contained AVS and AS samples. The microarray dataset was applied to identify differentially expressed genes (DEGs) by Limma. We also performed protein–protein interaction construction and machine learning to identify diagnostic genes which could mark AVS-AS progression. The efficacy of the diagnostic model was further validated using the RNA-sequencing dataset. We also analyzed the correlation between biomarkers and immune cells to understand changes in immune microenvironments during disease development. Finally, the expression levels of diagnostic genes were validated in normal, sclerotic, and stenotic valves using immunohistochemistry.

Materials and Methods

Data Resources and Clinical Samples

In this study, gene expression data for sclerotic and stenotic aortic valves were retrieved from the GEO database (https://www.ncbi.nlm.nih.gov/geo/). The GSE51472 dataset, which included both AVS (n = 5) and AS (n = 5) samples, was considered as the training cohort. The GSE138531 dataset, which also contained both AVS (n = 3) and AS (n = 3) samples, was used as the validation cohort.

Clinical samples were also obtained for further testing. The severity of aortic valve calcification was assessed by Doppler echocardiography and two-dimensional echocardiography. AS was characterized by leaflet stiffness, reduced leaflet motion and maximum aortic velocity over 2 m/s. Five stenotic aortic valves were acquired from patients with AS undergoing surgical aortic valve replacement. The criteria for SAVR in AS patients were patients with severe AS or with moderate AS undergoing coronary artery bypass grafting. SAVR can significantly relieve symptoms of cardiac insufficiency caused by AS and improve survival of patients. AVS was characterized by irregular thickening of leaflets and local echo enhancement. Five sclerotic aortic valves and five normal aortic valves were obtained from patients, with severe aortic valve prolapse undergoing surgical treatment. Valve replacement surgery can largely improve symptoms of cardiac dysfunction caused by valve prolapse. Patients with acute inflammation, such as the rheumatic valvular heart disease, endocarditis, and connective tissue diseases, such as syphilis, arteritis and Marfan syndrome were excluded from the study. All aortic valves were acquired from Ruijin Hospital, Shanghai Jiao Tong University School of Medicine (Shanghai, China). Study protocol was approved by the Ethics Committee of Ruijin Hospital, Shanghai Jiao Tong University School of Medicine, and written informed consent was obtained from all patients.

Identifying Differentially Expressed Genes

Log2 transformation was performed on the GSE51472 dataset. Principal component analysis (PCA) was conducted to examine heterogeneity between the AVS and AS groups. After annotation of probes, the Limma R package was used to perform DEG analysis between the AVS and AS samples. A heatmap plot was drawn with the pheatmap R package to present differential expressions of DEGs between sclerosis and stenosis. The criteria for DEGs were set as $|\log2(\text{fold change})| > 1$ and P value <0.05.

Enrichment Analysis

The conversion from gene symbol to Entrez ID for enrichment analysis was performed by the org.Hs.eg.db R package. Gene Ontology (GO) analysis involves three domains: biological process (BP), molecular function (MF), and cellular component (CC). GO and Kyoto Encyclopedia of Genes and Genomes (KEGG) pathway enrichment analyses were conducted using the ClusterProfiler R package. Bubble and the circle charts were created to visualize analysis of functions and pathways. Enrichment analysis was performed for DEGs, and node genes were selected using Cytoscape. The P value was adjusted by the Benjamini–Hochberg method. An adjusted P value <0.05 was set as the cut-off criterion.

Protein–Protein Interaction Network Construction

A protein–protein interaction (PPI) network of DEGs was constructed based on the String database (https://string-db.org). Cytoscape (Version 3.9.1) was applied to visualize the PPI network. The CytoNCA plug-in of Cytoscape was applied to analyze the betweenness centrality of genes. The cytoHubba plug-in was used to calculate protein node scores by the MCC algorithm. The top 5% of DEGs (n = 17) were identified for subsequent analysis. From the previous enrichment analysis, functions and pathways were related to the immune response. Therefore, immune-related genes were downloaded from the ImmPort Database. A Venn diagram was drawn to analyze interactions between these 17 nodes and immune genes.

Constructing a Diagnostic Model

Least absolute shrinkage and selection operator (LASSO) regression was applied to further filter candidate genes and identify diagnostic genes for predicting AVS progression to AS. LASSO regression is a method for variable selection and regularization to enhance the prediction accuracy and understanding of statistical models.[17] The GSE138531 dataset was used to validate the LASSO model. The LASSO model was constructed using the Glmnet R Package. The lambda.min and lambda.1se were calculated, and any lambda value between them was considered reasonable. The lambda.1se value was applied to select the smallest number of diagnostic genes in the appropriate range. Receiver operating characteristic (ROC) analysis was performed using the pROC package for both datasets to evaluate the efficacy of the model and each diagnostic gene. An area under the curve (AUC) >0.75 was regarded as having efficient diagnostic value.

Immune Infiltration Analysis

CIBERSORT is an analytical method to estimate abundances of cell types from tissue gene expression profiles.[18] Immune cell infiltration analysis was conducted to identify the immune cell proportion in AVS and AS using the Cibersort R package (https://cibersort.stanford.edu/index.php). A bar plot was applied to display the percentage of diverse immune cells in each sample. In addition, a boxplot was used to compare the proportions of 22 types of immune cells between the AVS and AS groups. Correlation analysis between diagnostic gene expressions and immune cell fractions was performed using the Hmisc package, and the results were displayed as charts using the ggplot R package.

Immunohistochemistry

Immunohistochemistry for valve tissues was performed as previously described.[19,20] The collected valve tissues were fixed overnight in 4% paraformaldehyde and then embedded in optimal cutting temperature compound. Tissues were sliced into 6-μm-thick frozen sections that were then stained with hematoxylin and eosin (H&E), Alizarin Red S, and Masson's trichrome stain for histological examination.

Expressions of IL-7 and VCAM-1 in valve tissues were measured by immunohistochemistry with rabbit polyclonal antibodies against IL-7 (1:200, Cat# ab175380, Abcam, MA, USA) and VCAM-1 (1:200, Cat# ab134047, Abcam, MA, USA). Then, sections were incubated with horseradish peroxidase (HRP)-conjugated secondary antibodies (1:500, Cat# 7076S, CST, MA, USA), followed by incubation with 3.3'-diaminobenzidine and counterstaining with hematoxylin. All sections were photographed with a microscope (Olympus Microsystems). Immunohistochemistry results were measured and analyzed by Image-Pro Plus software (v6.0; Media Cybernetics).

Statistical Analyses

Comparisons of continuous variables between two independent groups were conducted using a Student's *t*-test. Analysis of variance (ANOVA) was applied to analyze continuous variables among three independent groups. Chi-square test was used to analyze categorical variables. Correlation analysis was performed based on the Pearson correlation. $P < 0.05$ was considered statistically significant. R software (version 4.1.3) and SPSS Statistics (version 29.0.2) were used to conduct all analyses. Figure 1 was presented by Figdraw to illustrate possible role of diagnostic genes in CAVD progression.

Result

Identification and Functional Analysis of DEGs

Figure 2 shows the study flowchart. The significant difference between AVS samples and AS samples are shown in a PCA graph. The PCA graph of the first two components explained 42.5% of the variation, with the first principal component (PC1 or Dim1) accounting for 25.8% and the second (PC2 or Dim2) for 16.7% (Figure 3A). A total of 330 DEGs were identified in the GSE51472 dataset, including 92 downregulated genes and 238 upregulated genes. IL-7 and VCAM-1, genes identified as diagnostic genes in follow-up analysis, were both upregulated, with logFC values of 1.07 and 1.43, respectively. DEGs are visualized using a volcano plot (Figure 3B). Expressions of DEGs among samples are displayed by a heatmap (Figure 3C).

To further study the biological functions of the DEGs, GO and KEGG pathway enrichment analyses were conducted. GO analysis indicated that DEGs were significantly enriched in "leukocyte migration", "humoral immune response", and "cytokine activity." KEGG analysis showed that DEGs were primarily related to "viral protein interaction with cytokine and cytokine receptor" and "chemokine signaling pathway." The top 5 enriched terms of BP, CC, and MF are displayed in Figure 3D. The top 10 enriched KEGG pathways are presented in Figure 3E.

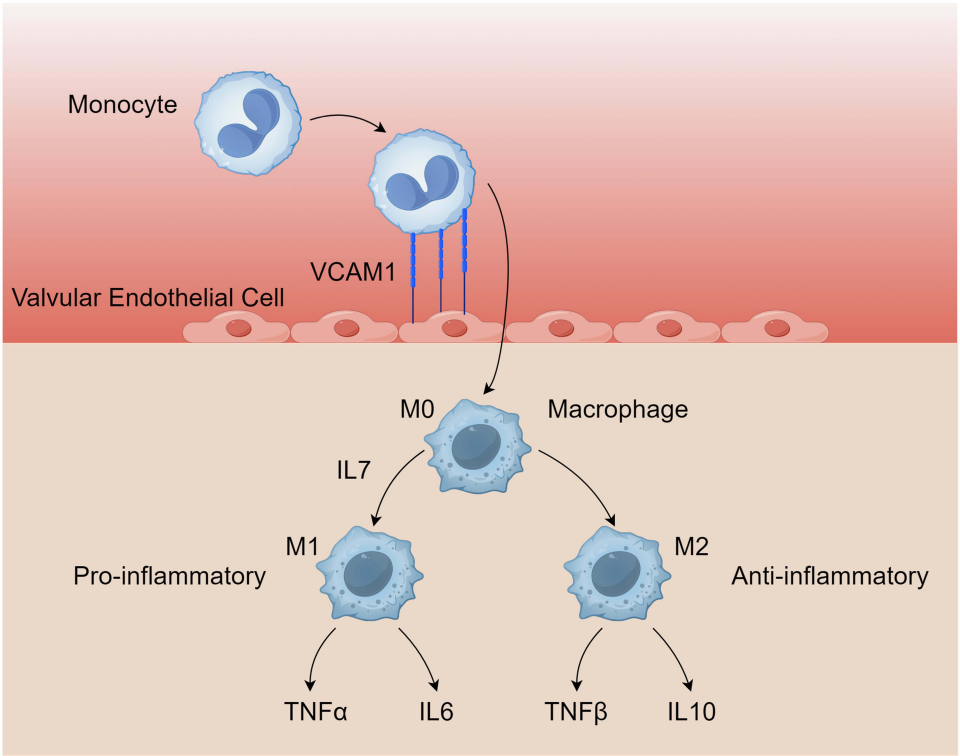

Figure 1 The possible mechanisms IL7 and VCAM1 involved in for the disease progression. The two diagnostic genes, IL7 and VCAM1 interact with immune cells to promote the progression from AVS to AS together. By Figdraw.

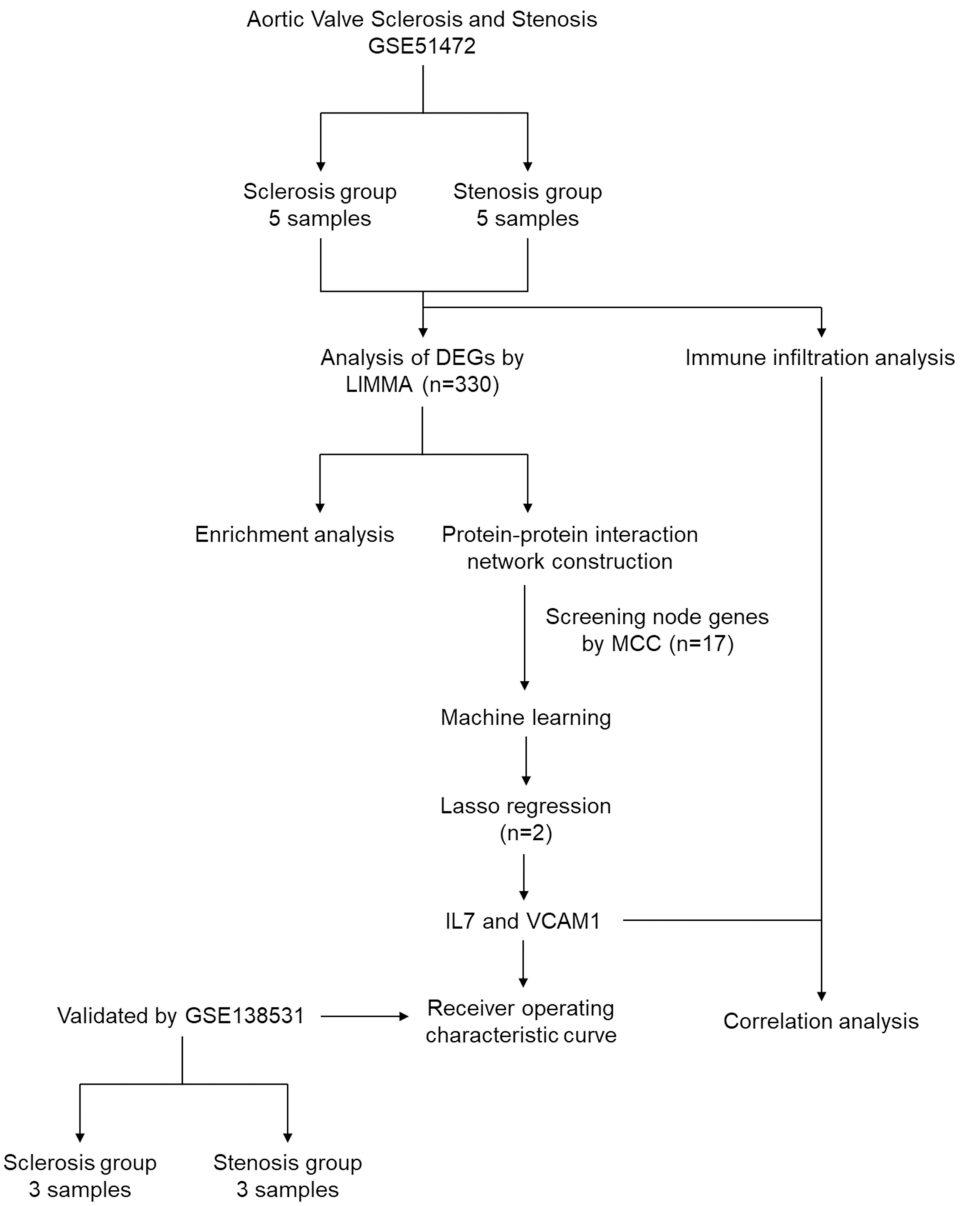

Figure 2 Study flowchart.
Abbreviations: GSE, Gene Expression Omnibus series; DEGs, differentially expressed genes; Limma, linear models for microarray data.

Node Gene Identification and Functional Analysis

A PPI network of DEGs was constructed using the STRING database and visualized by Cytoscape. Red dots represent upregulated genes and blue dots represent downregulated genes. Dot sizes represent the betweenness centrality of genes (Figure S1). Analysis of the CytoHubba plugin in Cytoscape identified the top 17 node genes (5% of DEGs), including IL-7 and VCAM-1, ranked by the MCC algorithm for subsequent analysis (Figure 4A). The Venn diagram showed that most of the node genes (88.2%) were immune-related genes, further validating immune microenvironment changes during the progression from AVS to AS (Figure 4B). GO and KEGG pathway enrichment analyses were then performed for node genes. GO analysis showed that the node genes were enriched in "positive regulation of response to external stimulus", "cytokine activity", and "chemokine activity." KEGG analysis illustrated that the node genes were mainly enriched in "cytokine–cytokine receptor interaction", "toll-like receptor (TLR) signaling pathway", and "chemokine signaling pathway." The top 5 enriched terms of BP, CC, and MF are shown in Figure 4C. The top 10 enriched KEGG pathways are shown in Figure 4D.

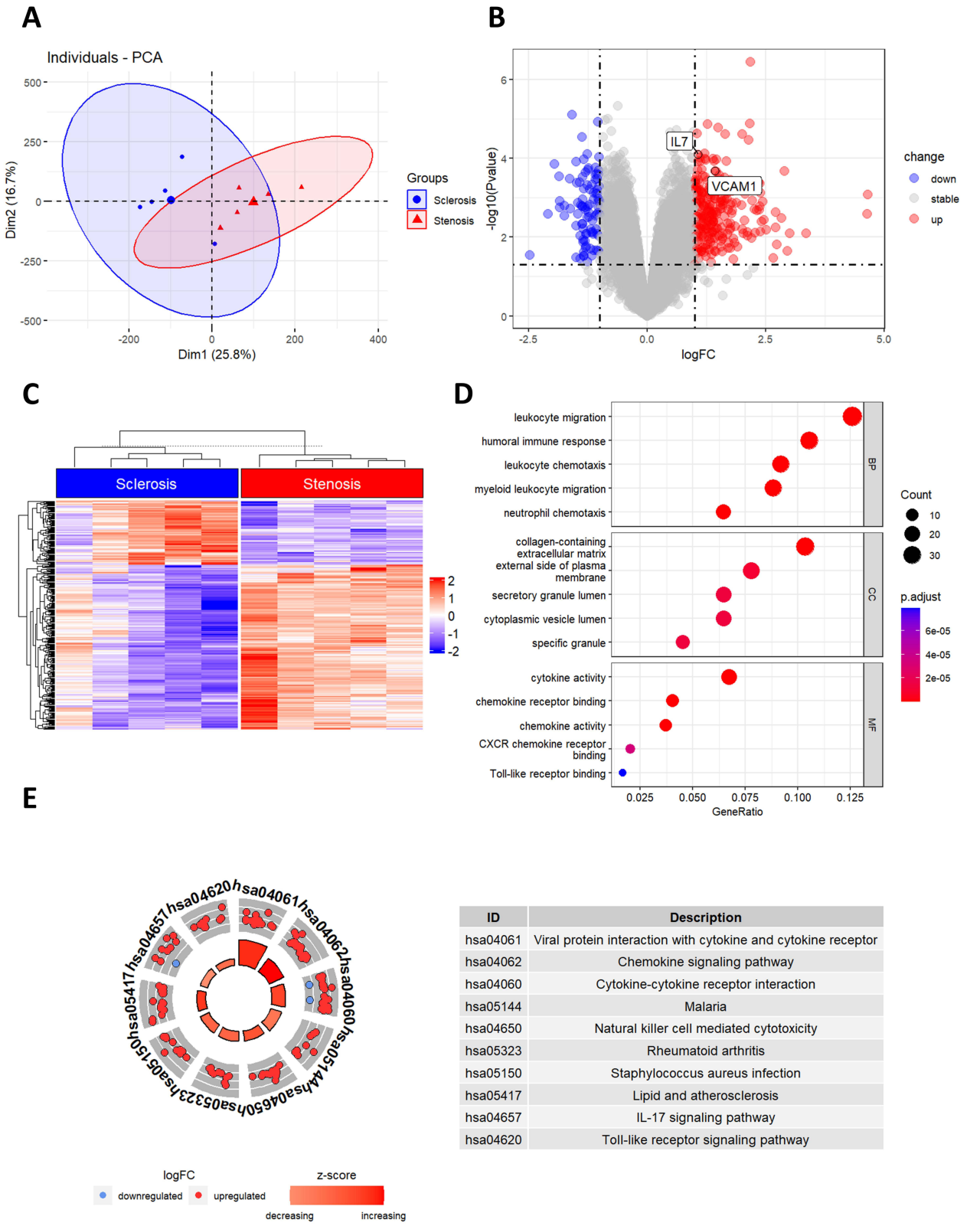

ID	Description
hsa04061	Viral protein interaction with cytokine and cytokine receptor
hsa04062	Chemokine signaling pathway
hsa04060	Cytokine-cytokine receptor interaction
hsa05144	Malaria
hsa04650	Natural killer cell mediated cytotoxicity
hsa05323	Rheumatoid arthritis
hsa05150	Staphylococcus aureus infection
hsa05417	Lipid and atherosclerosis
hsa04657	IL-17 signaling pathway
hsa04620	Toll-like receptor signaling pathway

Figure 3 Identification of DEGs between sclerotic and stenotic tissues and enrichment analysis of DEGs. (**A**) PCA for sclerotic and stenotic tissues. (**B**) Volcanic map of identified DEGs (P < 0.05, |logFC| > 1) between sclerotic and stenotic tissues. Red dots represent upregulated genes and blue dots represent downregulated genes. (**C**) Heatmap of DEGs. Upregulated genes are shown in red and downregulated genes are shown in blue. (**D**) The top five GO analysis results of DEGs. (**E**) KEGG pathway enrichment analysis results of DEGs (top 10 according to adjusted P value).

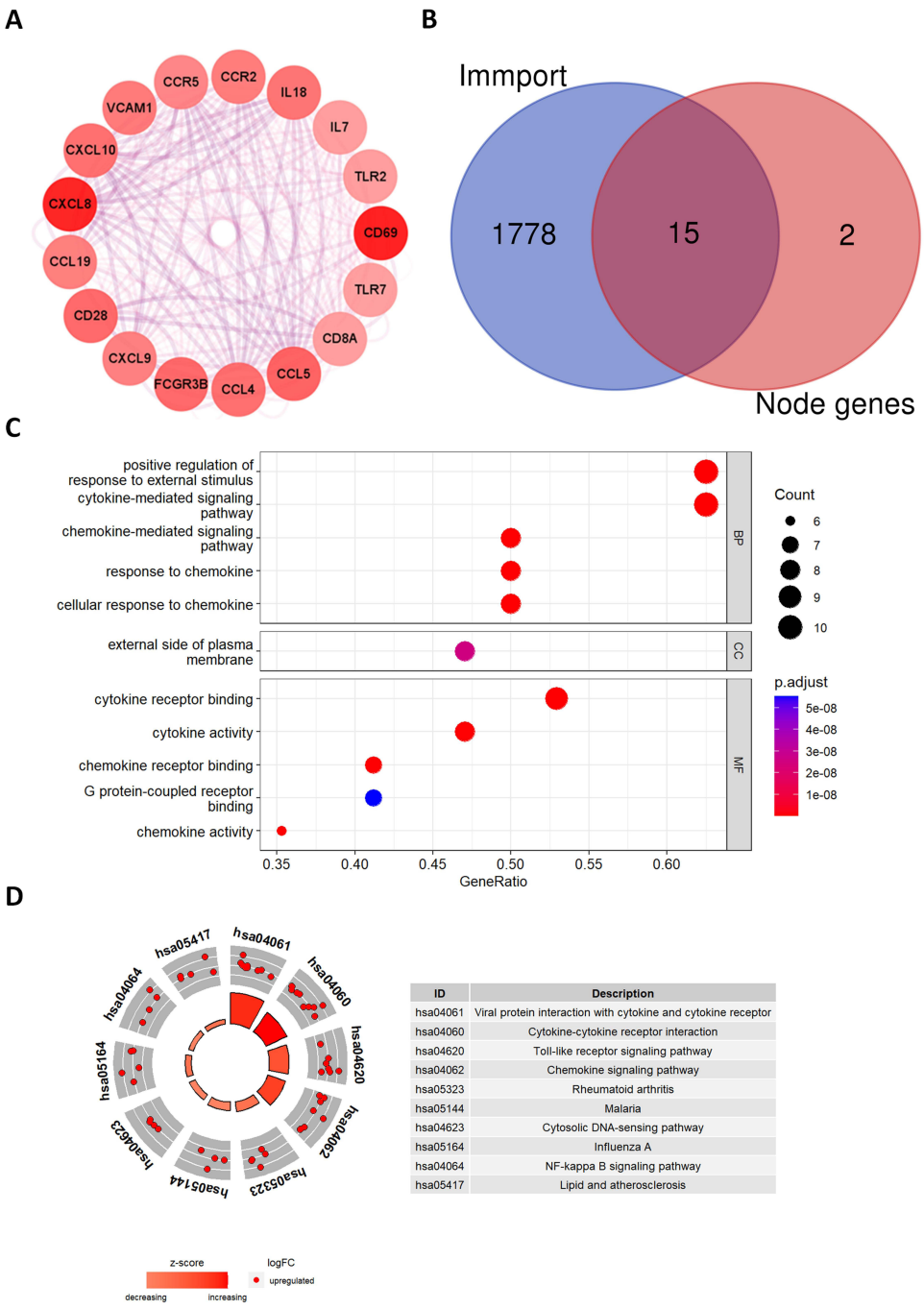

ID	Description
hsa04061	Viral protein interaction with cytokine and cytokine receptor
hsa04060	Cytokine-cytokine receptor interaction
hsa04620	Toll-like receptor signaling pathway
hsa04062	Chemokine signaling pathway
hsa05323	Rheumatoid arthritis
hsa05144	Malaria
hsa04623	Cytosolic DNA-sensing pathway
hsa05164	Influenza A
hsa04064	NF-kappa B signaling pathway
hsa05417	Lipid and atherosclerosis

Figure 4 Identification of node genes between sclerotic and stenotic tissues and enrichment analysis of node genes. (**A**) The top 17 node genes were identified from the PPI network. (**B**) Fifteen genes were identified from the interaction of node genes and immune-related genes were downloaded from ImmPort and placed in the Venn diagram. (**C**) The top five GO analysis results of node genes. (**D**) KEGG pathway enrichment analysis results of node genes (top 10 according to adjusted P value).

IL-7 and VCAM-1 as Diagnostic Genes via LASSO Regression

To identify diagnostic genes for AVS progression to AS, LASSO regression was performed to screen diagnostic biomarkers. Two genes, IL-7 and VCAM-1, were identified based on machine learning (Figure 5A and B). We then proceeded to analyze expressions of these two genes in the GSE138531 dataset. The median expression levels of IL-7 and VCAM-1 were both increased in AS samples compared to AVS samples, consistent with the expression pattern in the GSE51472 dataset (Figure 5C). ROC analysis was conducted to evaluate the sensitivity and specificity of the model and each gene. The AUC of the model constructed by LASSO regression was 1.00 for the training group and 0.78 for the

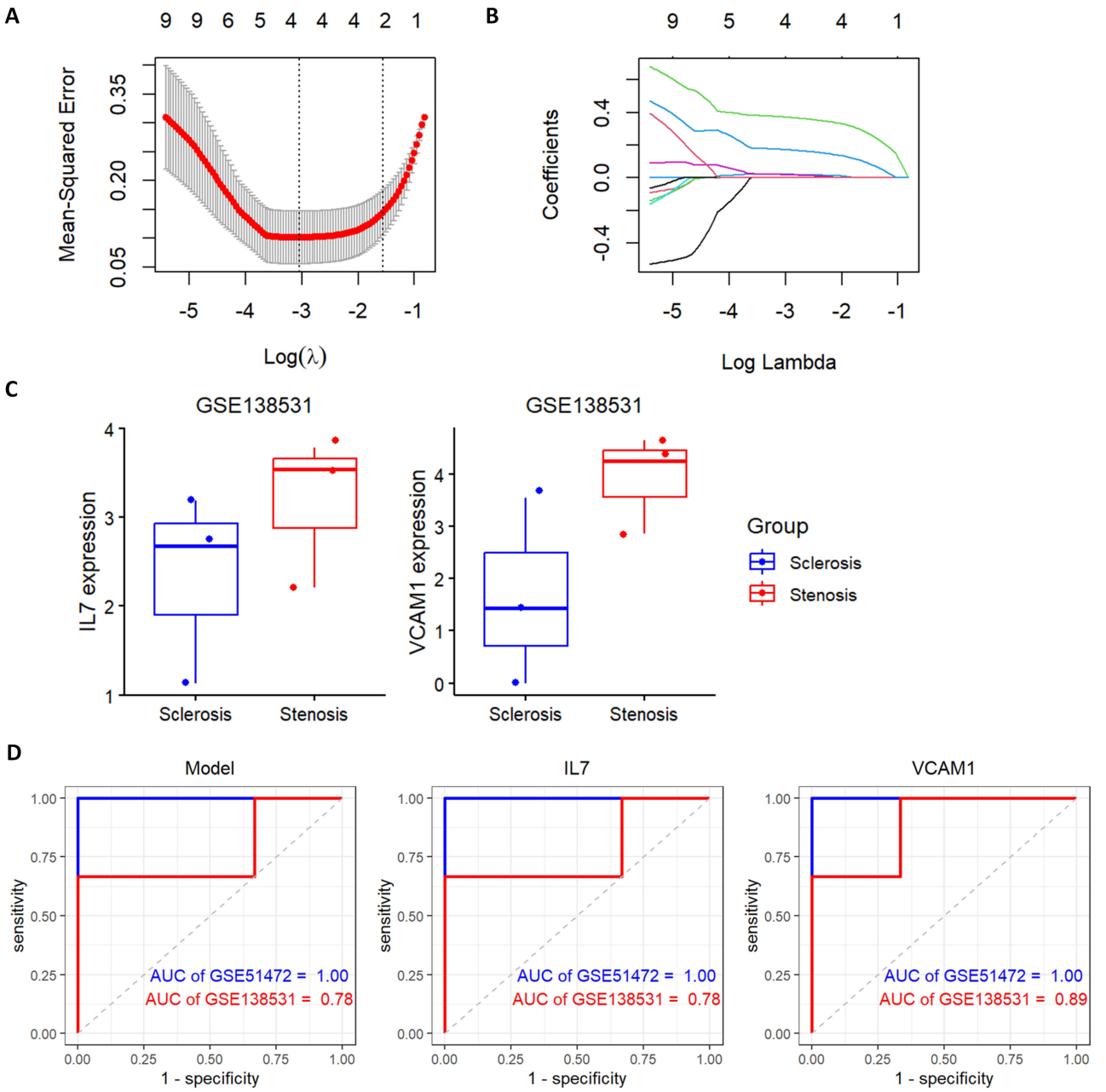

Figure 5 Construction of the diagnostic model. (**A** and **B**) LASSO regression was used to screen biomarkers. The dotted vertical lines show the optimal value through lambda.min and lambda.1 se. Diagnostic genes (n = 2) and their coefficients were selected according to lambda.1 se (**C**) Expression validations of the diagnostic genes IL-7 and VCAM-1 in the GSE138531 dataset. (**D**) ROC analysis of the diagnostic model; IL-7 and VCAM-1 in the GSE51472 dataset and GSE138531 dataset.

validation group, which indicated that the diagnostic model possessed a high ability to differentiate AVS samples from AS samples (Figure 5D). In addition, the diagnostic value for each gene (IL-7 or VCAM-1) was also strong (Figure 5D).

Immune Cell Infiltration Analysis

Our enrichment analysis revealed that DEGs were primarily enriched via the inflammatory response and immune regulation. Thus, immune cell infiltration analysis was conducted to better elucidate changes in the immune microenvironment during the progression from AVS to AS. A bar plot shows the proportion of 22 types of immune cells in different samples (Figure 6A). Furthermore, comparison of immune cell proportions between AVS and AS was revealed. The proportion of M2 macrophages was significantly lower in the AS group than in the AVS group, while the percentages of

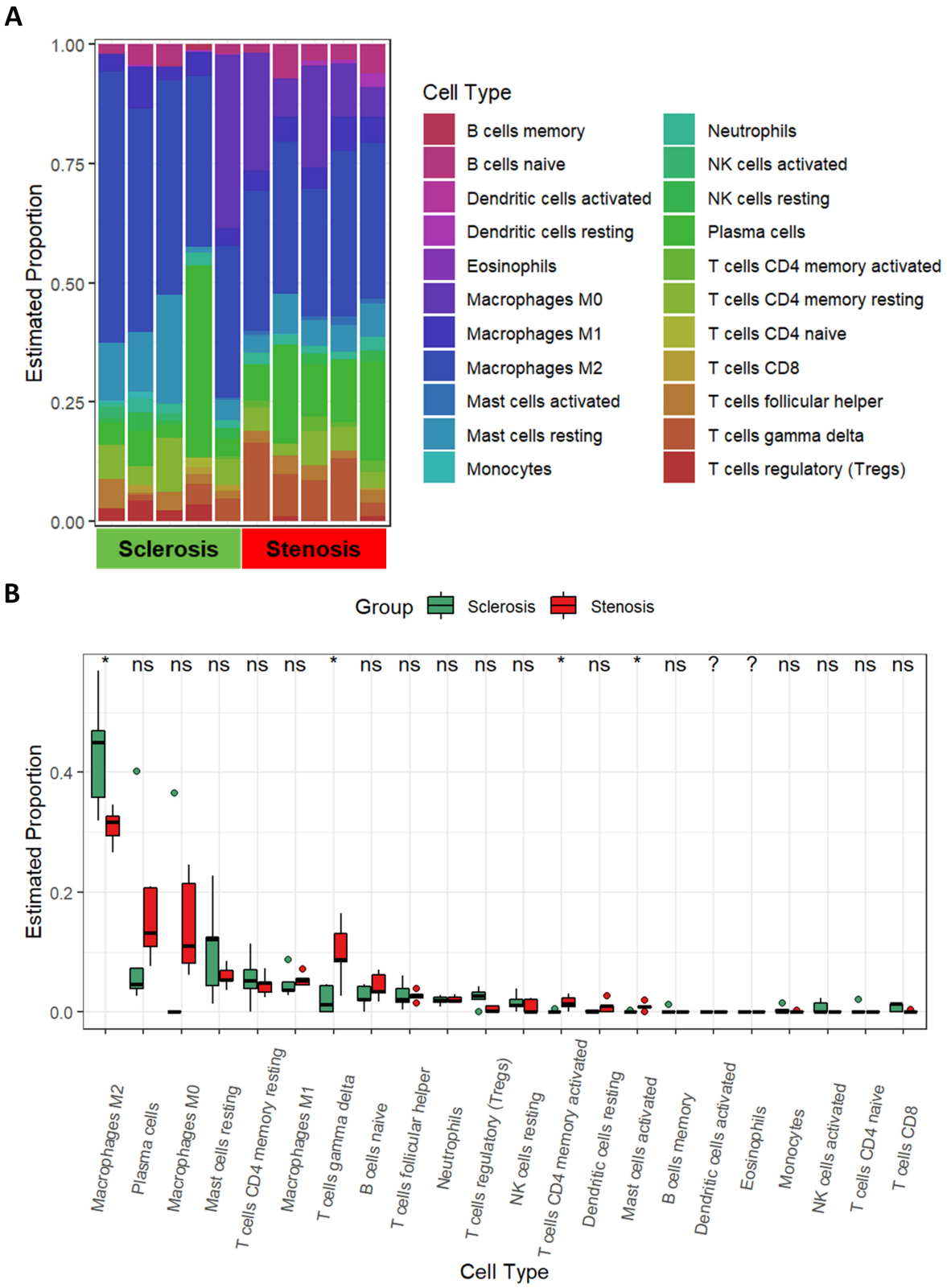

Figure 6 Immune cell infiltration analysis between AS and AVS. (**A**) The proportion of 22 immune cells in sclerotic and stenotic valves visualized by a bar plot. (**B**) Differences in immune infiltration between the AVS and AS groups. *P < 0.05. ns: P > 0.05. ?: The calculated proportion = 0 in both sclerosis and stenosis group.

gamma-delta T cells, activated CD4 memory T cells, and activated mast cells were distinctly increased in the AS group (Figure 6B).

Correlation Analysis of IL-7 and VCAM-1 with Infiltrated Immune Cells

To reveal the relationship of IL-7 and VCAM-1 with immune cells, Pearson correlation analysis was performed (Figure 7A). IL-7 was positively related to activated mast cells (r = 0.83), gamma-delta T cells (r = 0.75), and activated CD4 memory T cells (r = 0.73) but negatively associated with M2 macrophages (r = −0.70) and regulatory T cells (r = −0.81) (Figure 7B and C). VCAM-1 was also positively related to gamma-delta T cells (r = 0.68) but negatively with M2 macrophages (r = −0.74) and regulatory T cells (r = −0.64; Figure 7B and D).

Validation the Expression Differences of IL-7 and VCAM-1

Immunohistochemistry was conducted to further validate expressions of diagnostic genes in normal, sclerotic, and stenotic aortic valves. The clinical characteristics was shown in Table 1. The demographic features and comorbidities did not differ between the sclerosis group and the stenosis group. Patients with AS tended to have higher levels of TC and LDL than AVS patients and normal people. Immunohistochemistry results showed that the expression levels of IL-7 and VCAM-1 were highest in the stenotic valves, which was consistent with the above dataset results (Figure 8A and B).

Discussion

AS is the most prevalent valvular disease in developed countries and is the second most frequent cause of cardiac surgery.[21,22] The mechanisms of the disease progression from AVS to AS are still not fully understood. Our study is the first to identify diagnostic biomarkers and analyze inflammatory microenvironmental changes during the progression from AVS to AS. We found that IL-7 and VCAM-1, as core regulatory genes, presented strong diagnostic value. Revealing biomarkers during the progression can be helpful in the search for new therapeutic targets preventing or slowing disease development. In addition, building a model to diagnose disease state and provide proper medical interventions in a timely fashion is also crucial to improve AS prognosis.

Our research found that the process by which AVS developed to AS included 330 DEGs. GO analysis showed that the DEGs were primarily enriched in immune responses, such as leukocyte migration, leukocyte chemotaxis, and chemokine activities. KEGG analysis also indicated that DEGs were mainly enriched in immune-related pathways, such as chemokine and TLR signaling pathways. TLR signaling pathways were reported to activate NF-κB signaling pathways, the latter participating in AS pathogenesis.[23,24] These results illustrated that inflammatory responses not only affected the pathological process of AVS or AS alone but also participated in the progression from AVS to AS. The top 17 node genes (5% of DEGs) were then identified following the PPI network construction, with 15/17 node genes being immune-related genes enriched in immune pathways. Moreover, LASSO regression analysis of these node genes identified IL-7 and VCAM-1 as diagnostic genes for the progression of AS from AVS. The model and each identified gene presented good diagnostic value in both the training and the validation groups (AUC value > 0.75).

IL-7 is a secreted soluble globular protein belonging to the gamma-chain cytokine family.[25] IL-7 participates in several cardiovascular diseases. IL-7 was reported to promote myocardial I/R injury.[26] Further, anti-IL-7 antibodies have been reported to reduce myocardial infarction area through suppression of macrophage infiltration and decreasing M1/M2 macrophage ratios.[26] IL-7 drives the expansion of pro-inflammatory CD28null T cells in acute coronary syndrome, and Tofacitinib, an IL-7 blockade, can prevent immune cell expansion, thereby improving outcomes.[27] IL-7 also contributes to atherosclerosis through activation of NF-κB signaling pathways and recruitment of macrophages to adhere to endothelial cells.[28] Previous research has found that neutrophils produce IL-7 under stimulation of rising levels of lipids during the progression of AS.[13] Our results also showed that expression of IL-7 was higher in stenotic valves than in sclerotic and normal valves. However, the role of IL-7 in AS development has not been explored. As the mechanism of atherosclerosis and AS share a certain similarity, based on our results, we speculated that IL-7 also participated in the progression from AVS to AS.[13,29]

VCAM-1, an immunoglobulin (Ig) superfamily member, is expressed by endothelial cells, mediating monocyte adhesion.[30] VCAM-1 contributes to several cardiac diseases, including atrial fibrillation and heart failure.[31,32] VCAM-1 has also been reported to promote atherosclerosis by inducing monocytes to infiltrate subendothelial spaces and therefore

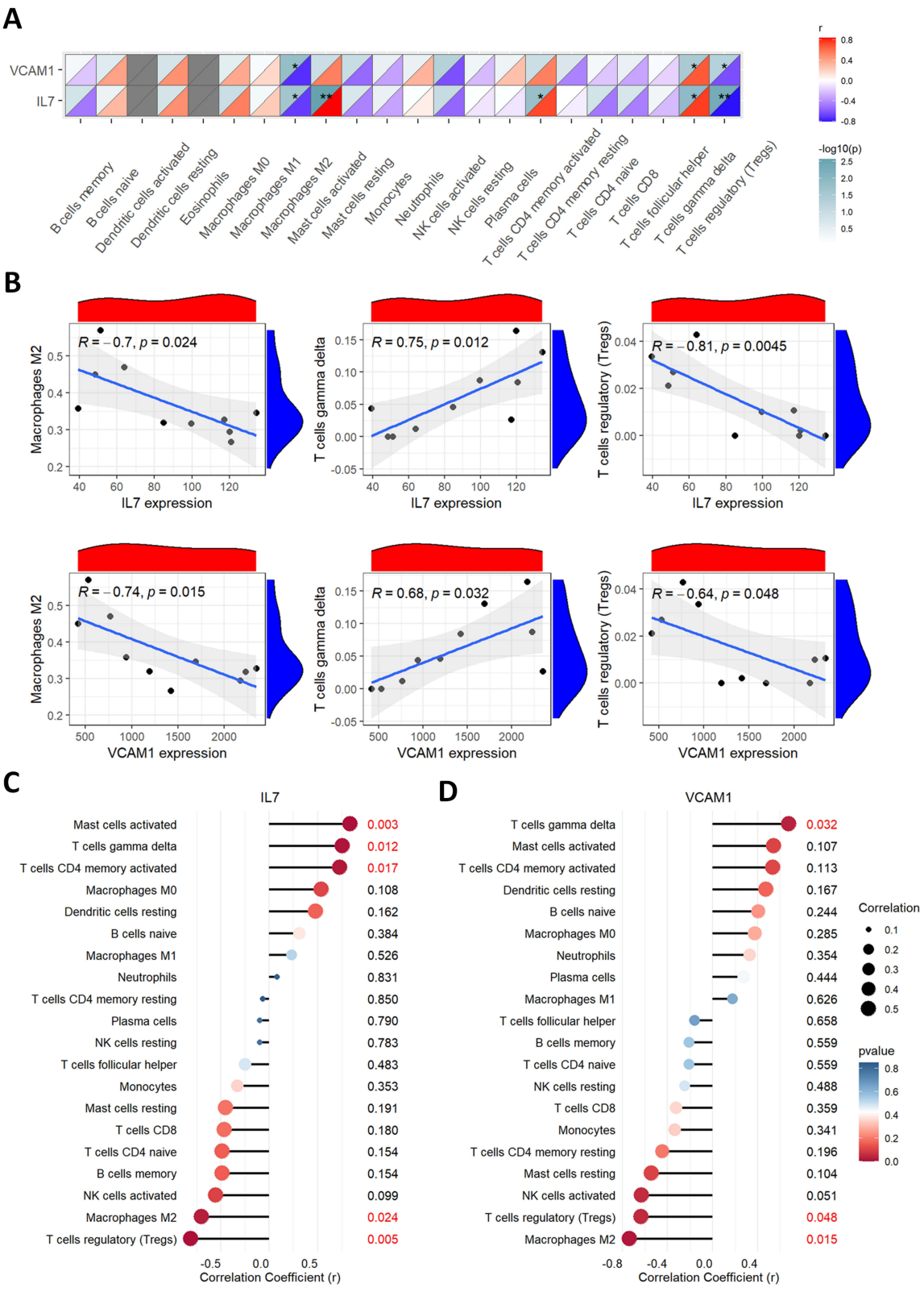

Figure 7 Correlation analysis between IL-7 and VCAM-1 expression and immune cell infiltration. (**A**) Correlation analysis visualized using a heatmap. (**B**) Correlation analysis. (**C**) Bubble chart of correlations between IL-7 expressions and immune cell proportions. (**D**) Bubble chart of correlations between VCAM-1 expression and immune cell proportions. *P < 0.05. **P < 0.01.

Table 1 Clinical Characteristics of Normal People and Patients with AVS and as

	Normal (n=5)	Sclerosis (n=5)	Stenosis (n=5)	P value	P value (Sclerosis vs Stenosis)
Age, y, mean (SD)	49.20 (44.38–54.22)	79.40 (75.89–82.91)	70.40 (60.54–80.26)	<0.001	0.091
Male, n (%)	3 (60%)	3 (60%)	4 (80%)	1	1
BMI, kg/m², median (IQR)	24.95 (23.26–26.64)	25.18 (21.55–28.81)	26.03 (23.60–28.46)	0.806	0.675
Drinking, n (%)	1 (20%)	0 (0%)	2 (40%)	0.725	0.444
Smoking, n (%)	1 (20%)	0 (0%)	1 (20%)	1	1
HbA1c, %, mean (SD)	5.96 (5.46–6.46)	6.56 (5.27–7.85)	6.88 (5.84–7.93)	0.367	0.677
TG, mmol/L, median (IQR)	1.51 (0.80–2.22)	1.67 (0.77–2.57)	2.24 (1.32–3.16)	0.386	0.348
TC, mmol/L, median (IQR)	3.08 (2.75–3.41)	2.78 (2.30–3.26)	4.85 (4.43–5.27)	<0.001	<0.001
HDL, mmol/L, median (IQR)	0.98 (0.85–1.12)	0.98 (0.67–1.30)	0.95 (0.80–1.11)	0.964	0.843
LDL, mmol/L, median (IQR)	1.73 (1.50–1.96)	1.39 (1.03–1.75)	3.20 (2.85–3.56)	<0.001	<0.001
Lp (a), mmol/L, median (IQR)	0.14 (0.10–0.18)	0.19 (0.01–0.37)	0.26 (0.05–0.46)	0.508	0.592
Comorbid condition					
Diabetes, n (%)	2 (40%)	2 (40%)	3 (60%)	1	1
Hypertension, n (%)	2 (40%)	5 (100%)	4 (80%)	0.231	1
CAD, n (%)	4 (80%)	5 (100%)	4 (80%)	1	1

Abbreviations: BMI, Body mass index; HbA1c, Hemoglobin A1C; TG, Triglycerides; TC, Total cholesterol; HDL, High-density lipoprotein; LDL, Low-density lipoprotein; Lp (a), Lipoprotein (a); SD, Standard deviation; IQR, Interquartile range.

became a popular therapeutic target.[33] Currently, several VCAM-1-inhibiting drugs for atherosclerosis are under pre-clinical or clinical research.[34] Our results found that expressions of VCAM-1 were higher in stenotic valves than in sclerotic valves. Previous studies have indicated that VCAM-1 plays an active role in AS pathogenesis.[13] Similar to the pathological process of atherosclerosis, NF-κB stimulates VCAM-1 production in VECs.[35] VCAM-1 attracts leukocytes into valves and is necessary for the formation of inflammatory lesions.[21,35] The crucial roles of VCAM-1 make it a potential target to prevent the progression from AVS to AS.

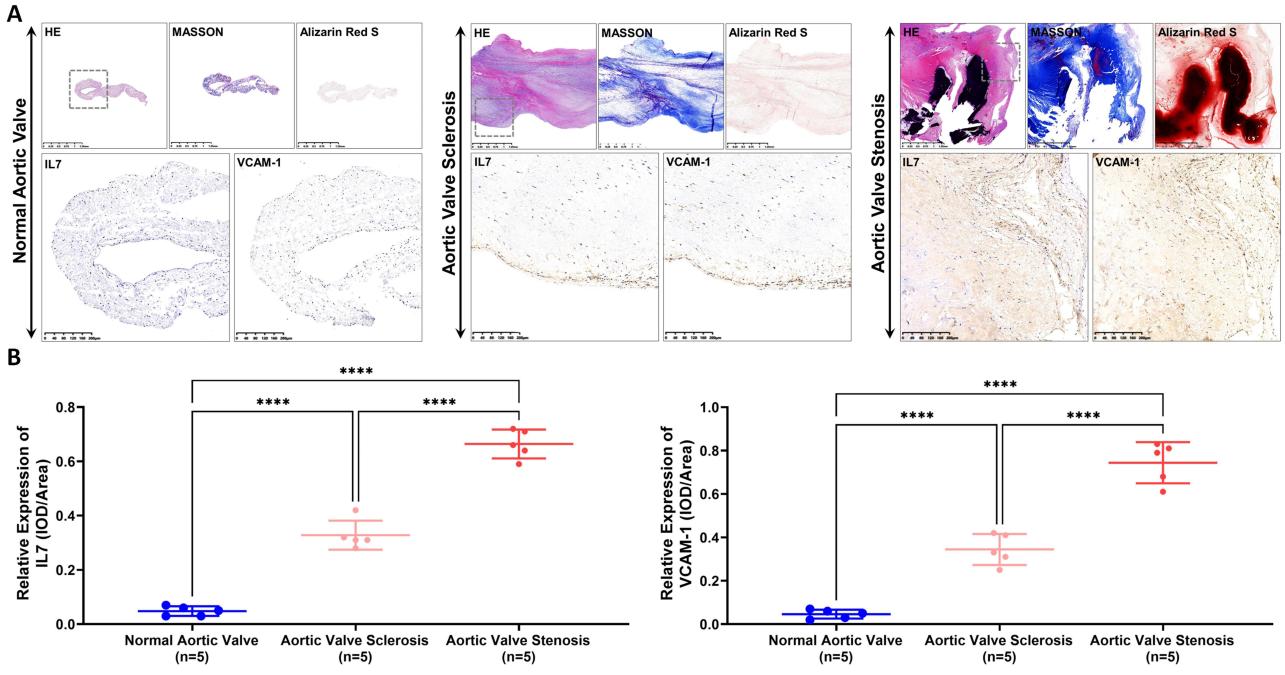

Figure 8 Levels of IL-7 and VCAM-1 in normal, sclerotic, and stenotic valves. (**A**) hematoxylin-eosin (HE), Masson, and alizarin red staining revealed the highest levels of IL-7 and VCAM-1 in stenotic aortic valves and relatively higher expressions of IL-7 and VCAM-1 in sclerotic aortic valves than in normal aortic valves (bar = 50 μm). (**B**) Quantification of IL-7 and VCAM-1 expression among the three groups. ****P < 0.0001.

The amount and phenotype of immune cells also play key roles in regulating the immune microenvironment during disease progression. Our correlation analysis suggests that IL-7 and VCAM-1 are negatively related to M2 macrophages but positively associated with gamma-delta T cells. Macrophages, derived from monocytes, infiltrate valves via adhesion molecules, such as VCAM-1, and differentiate into pro-inflammatory M1 macrophages and anti-inflammatory M2 macrophages.[36,37] The balance of M1/M2 was found to be dysfunctional in our results, with the proportion of M2 macrophages significantly diminished and that of M1 macrophages elevated in stenotic valves, further demonstrating more intense immune responses in AS than in AVS. Gamma-delta T cells have been reported to promote cardiovascular diseases, such as atherosclerosis.[13] The levels of gamma-delta T cells were higher in stenotic valves based on our study. More research needed to elucidate the role gamma-delta T cells play during the development of AS. Proliferation of gamma-delta T cells has been reported to exclusively rely on IL-7.[38] Further, IL-7 has been reported to regulate the homeostasis and inflammatory responses of gamma-delta T cells.[39] These findings indicate that IL-7 and VCAM-1 can regulate the amount and proportion of immune cells to aggravate inflammatory responses and promote the progression of AVS to AS, which also supports the diagnostic value of IL-7 and VCAM-1 for the advancement of AVS to AS.

To the best of our knowledge, this is the first study to construct a diagnostic model of AVS to AS progression. Furthermore, our study demonstrated a positive correlation between the two diagnostic genes and pro-inflammatory immune cells. Despite these strengths, some limitations exist in this study. First, clinical characteristics of GEO datasets were not included in the analysis because it was difficult to obtain the information. Second, we identified IL-7 and VCAM-1 as diagnostic genes and validated their expression in sclerotic and stenotic valves using immunohistochemistry; however, the mechanism of targeted genes during disease development is worth further investigation through biological experiments.

Conclusion

In summary, we identified two diagnostic genes, IL-7 and VCAM-1, that were significantly associated with the disease progression from AVS to AS. Our results provide novel insights for investigating different expression patterns between sclerotic and stenotic valves in future studies. The two biomarkers and pro-inflammatory microenvironment in stenosis valves can also serve as novel potential targets in efforts to prevent disease progression. More datasets and in vivo studies are needed to further explore the significance of the two diagnostic genes in the disease progression.

Data Sharing Statement

The raw data supporting the conclusions of the current study will be made available from the corresponding author, Ke Yang.

Ethical Approval and Consent to Participate

The study protocol was approved by the Ethics Committee of Ruijin Hospital, Shanghai Jiao Tong University School of Medicine and was performed under the Declaration of Helsinki. Written informed consent was obtained from all patients.

Acknowledgments

We acknowledge The Charlesworth Group (https://charlesworth.com.cn/) for reviewing the manuscript for grammar consistency.

We would like to thank Dr. Ying Huang and her associates in the core facility unit (School of Medicine, Shanghai Jiao Tong University) for their professional support in imaging capture and processing.

Author Contributions

All authors made a significant contribution to the work reported, whether that is in the conception, study design, execution, acquisition of data, analysis and interpretation, or in all these areas; took part in drafting, revising or critically reviewing the article; gave final approval of the version to be published; have agreed on the journal to which the article has been submitted; and agree to be accountable for all aspects of the work.

Funding

This work was supported by grants from the National Natural Science Foundation of China (82070401) and sponsored by the Shanghai Pujiang Program (22PJD044).

Disclosure

The authors report no conflicts of interest in this work.

References

1. Otto CM, Nishimura RA, Bonow RO, et al. 2020 ACC/AHA guideline for the management of patients with valvular heart disease: executive summary: a report of the American college of cardiology/American heart association joint committee on clinical practice guidelines. *Circulation*. 2021;143(5):e35–e71. doi:10.1161/cir.0000000000000932
2. Poggio P, Sainger R, Branchetti E, et al. Noggin attenuates the osteogenic activation of human valve interstitial cells in aortic valve sclerosis. *Cardiovasc Res*. 2013;98(3):402–410. doi:10.1093/cvr/cvt055
3. Faggiano P, Antonini-Canterin F, Erlicher A, et al. Progression of aortic valve sclerosis to aortic stenosis. *Am J Cardiol*. 2003;91(1):99–101. doi:10.1016/s0002-9149(02)03011-4
4. Coffey S, Cox B, Williams MJ. The prevalence, incidence, progression, and risks of aortic valve sclerosis: a systematic review and meta-analysis. *J Am Coll Cardiol*. 2014;63(25):2852–2861. doi:10.1016/j.jacc.2014.04.018
5. Zilberszac R, Gabriel H, Schemper M, Laufer G, Maurer G, Rosenhek R. Asymptomatic severe aortic stenosis in the elderly. *JACC Cardiovasc Imaging*. 2017;10(1):43–50. doi:10.1016/j.jcmg.2016.05.015
6. Toff WD, Hildick-Smith D, Kovac J, et al. Effect of transcatheter aortic valve implantation vs surgical aortic valve replacement on all-cause mortality in patients with aortic stenosis: a randomized clinical Trial. *JAMA*. 2022;327(19):1875–1887. doi:10.1001/jama.2022.5776
7. Jørgensen TH, Thyregod HGH, Ihlemann N, et al. Eight-year outcomes for patients with aortic valve stenosis at low surgical risk randomized to transcatheter vs. surgical aortic valve replacement. *Eur Heart J*. 2021;42(30):2912–2919. doi:10.1093/eurheartj/ehab375
8. Ando T, Ashraf S, Villablanca PA, et al. Meta-analysis comparing the incidence of infective endocarditis following transcatheter aortic valve implantation versus surgical aortic valve replacement. *Am J Cardiol*. 2019;123(5):827–832. doi:10.1016/j.amjcard.2018.11.031
9. Rezk M, Taha A, Nielsen SJ, et al. Associations between new-onset postoperative atrial fibrillation and long-term outcome in patients undergoing surgical aortic valve replacement. *Eur J Cardiothorac Surg*. 2023;63(5). doi:10.1093/ejcts/ezad103
10. Seo JH, Chun KJ, Lee BK, Cho BR, Ryu DR. Statins have no role in preventing the progression of aortic valve sclerosis. *J Cardiovasc Imaging*. 2018;26(4):229–237. doi:10.4250/jcvi.2018.26.e27
11. Chan KL, Teo K, Dumesnil JG, Ni A, Tam J. Effect of Lipid lowering with rosuvastatin on progression of aortic stenosis: results of the aortic stenosis progression observation: measuring effects of rosuvastatin (ASTRONOMER) trial. *Circulation*. 2010;121(2):306–314. doi:10.1161/circulationaha.109.900027
12. Dweck MR, Jones C, Joshi NV, et al. Assessment of valvular calcification and inflammation by positron emission tomography in patients with aortic stenosis. *Circulation*. 2012;125(1):76–86. doi:10.1161/circulationaha.111.051052
13. Bartoli-Leonard F, Zimmer J, Aikawa E. Innate and adaptive immunity: the understudied driving force of heart valve disease. *Cardiovasc Res*. 2021;117(13):2506–2524. doi:10.1093/cvr/cvab273
14. Wang D, Xiong T, Yu W, et al. Predicting the key genes involved in aortic valve calcification through integrated bioinformatics analysis. *Front Genet*. 2021;12:650213. doi:10.3389/fgene.2021.650213
15. Liu C, Liu R, Cao Z, et al. Identification of MMP9 as a novel biomarker to mitochondrial metabolism disorder and oxidative stress in calcific aortic valve stenosis. *Oxid Med Cell Longev*. 2022;2022:3858871. doi:10.1155/2022/3858871
16. Zhou Y, Shi W, Zhao D, Xiao S, Wang K, Wang J. Identification of immune-associated genes in diagnosing aortic valve calcification with metabolic syndrome by integrated bioinformatics analysis and machine learning. *Front Immunol*. 2022;13:937886. doi:10.3389/fimmu.2022.937886
17. Yang C, Delcher C, Shenkman E, Ranka S. Machine learning approaches for predicting high cost high need patient expenditures in health care. *Biomed Eng Online*. 2018;17(Suppl 1):131. doi:10.1186/s12938-018-0568-3
18. Newman AM, Liu CL, Green MR, et al. Robust enumeration of cell subsets from tissue expression profiles. *Nat Methods*. 2015;12(5):453–457. doi:10.1038/nmeth.3337
19. Zhang Q, Ye J, Yang G, et al. Role of follistatin-like 1 levels and functions in calcific aortic stenosis. *Front Cardiovasc Med*. 2022;9:1050310. doi:10.3389/fcvm.2022.1050310
20. Chen Z, Shen Y, Xue Q, et al. Clinical relevance of plasma endogenous tissue-plasminogen activator and aortic valve sclerosis: performance as a diagnostic biomarker. *Front Cardiovasc Med*. 2020;7:584998. doi:10.3389/fcvm.2020.584998
21. Boskovski MT, Gleason TG. Current Therapeutic Options in Aortic Stenosis. *Circ Res*. 2021;128(9):1398–1417. doi:10.1161/circresaha.121.318040
22. Tornos P. [New aspects in aortic valve disease]. Nuevos aspectos de la valvulopatía aórtica. *Rev Esp Cardiol*. 2001;54(1):17–21. Spanish.
23. Gee T, Farrar E, Wang Y, et al. NFκB (Nuclear Factor κ-Light-Chain Enhancer of Activated B Cells) activity regulates cell-type-specific and context-specific susceptibility to calcification in the aortic valve. *Arterioscler Thromb Vasc Biol*. 2020;40(3):638–655. doi:10.1161/atvbaha.119.313248
24. Meng X, Ao L, Song Y, et al. Expression of functional Toll-like receptors 2 and 4 in human aortic valve interstitial cells: potential roles in aortic valve inflammation and stenosis. *Am J Physiol Cell Physiol*. 2008;294(1):C29–35. doi:10.1152/ajpcell.00137.2007
25. Barata JT, Durum SK, Seddon B. Flip the coin: IL-7 and IL-7R in health and disease. *Nat Immunol*. 2019;20(12):1584–1593. doi:10.1038/s41590-019-0479-x
26. Yan M, Yang Y, Zhou Y, et al. Interleukin-7 aggravates myocardial ischaemia/reperfusion injury by regulating macrophage infiltration and polarization. *J Cell Mol Med*. 2021;25(21):9939–9952. doi:10.1111/jcmm.16335

27. Bullenkamp J, Mengoni V, Kaur S, et al. Interleukin-7 and interleukin-15 drive CD4+CD28null T lymphocyte expansion and function in patients with acute coronary syndrome. *Cardiovasc Res*. 2021;117(8):1935–1948. doi:10.1093/cvr/cvaa202
28. Li R, Paul A, Ko KW, et al. Interleukin-7 induces recruitment of monocytes/macrophages to endothelium. *Eur Heart J*. 2012;33(24):3114–3123. doi:10.1093/eurheartj/ehr245
29. Wolf D, Ley K. Immunity and Inflammation in Atherosclerosis. *Circ Res*. 2019;124(2):315–327. doi:10.1161/circresaha.118.313591
30. Furuta K, Guo Q, Pavelko KD, et al. Lipid-induced endothelial vascular cell adhesion molecule 1 promotes nonalcoholic steatohepatitis pathogenesis. *J Clin Invest*. 2021;131(6). doi:10.1172/JCI143690
31. Willeit K, Pechlaner R, Willeit P, et al. Association Between Vascular Cell Adhesion Molecule 1 and Atrial Fibrillation. *JAMA Cardiol*. 2017;2(5):516–523. doi:10.1001/jamacardio.2017.0064
32. Patel RB, Colangelo LA, Bielinski SJ, et al. Circulating vascular cell adhesion molecule-1 and incident heart failure: the multi-ethnic study of atherosclerosis (Mesa). *J Am Heart Assoc*. 2020;9(22):e019390. doi:10.1161/jaha.120.019390
33. Ley K, Huo Y. VCAM-1 is critical in atherosclerosis. *J Clin Invest*. 2001;107(10):1209–1210. doi:10.1172/jci13005
34. Pickett JR, Wu Y, Zacchi LF, Ta HT. Targeting endothelial vascular cell adhesion molecule-1 in atherosclerosis: drug discovery and development of vascular cell adhesion molecule-1-directed novel therapeutics. *Cardiovasc Res*. 2023;119(13):2278–2293. doi:10.1093/cvr/cvad130
35. Driscoll K, Cruz AD, Butcher JT. Inflammatory and biomechanical drivers of endothelial-interstitial interactions in calcific aortic valve disease. *Circ Res*. 2021;128(9):1344–1370. doi:10.1161/circresaha.121.318011
36. Li G, Qiao W, Zhang W, Li F, Shi J, Dong N. The shift of macrophages toward M1 phenotype promotes aortic valvular calcification. *J Thorac Cardiovasc Surg*. 2017;153(6):1318–1327.e1. doi:10.1016/j.jtcvs.2017.01.052
37. Domschke G, Gleissner CA. CXCL4-induced macrophages in human atherosclerosis. *Cytokine*. 2019;122:154141. doi:10.1016/j.cyto.2017.08.021
38. Bekiaris V, Šedý JR, Macauley MG, Rhode-Kurnow A, Ware CF. The inhibitory receptor BTLA controls γδ T cell homeostasis and inflammatory responses. *Immunity*. 2013;39(6):1082–1094. doi:10.1016/j.immuni.2013.10.017
39. Corpuz TM, Stolp J, Kim HO, et al. Differential Responsiveness of Innate-like IL-17- and IFN-γ-Producing γδ T cells to homeostatic cytokines. *J Immunol*. 2016;196(2):645–654. doi:10.4049/jimmunol.1502082